**RAA 2019** Vol. **19** No. **5**, 68(8pp) doi: 10.1088/1674–4527/19/5/68

*http://www.raa-journal.org* *http://iopscience.iop.org/raa*

*Research in Astronomy and Astrophysics*

# Local standard of rest based on *Gaia* DR2 catalog

Ping-Jie Ding, Zi Zhu and Jia-Cheng Liu

School of Astronomy and Space Science, Nanjing University, Nanjing 210023, China; *zhuzi@nju.edu.cn*
Key Laboratory of Modern Astronomy and Astrophysics (Nanjing University), Ministry of Education, Nanjing 210023, China

Received 2018 September 14; accepted 2018 November 3

**Abstract** The local standard of rest (LSR) provides a reference framework for studies of Galactic kinematics. Determination of the LSR corresponds to the measurement of solar peculiar motion, which is under debate due to the fact that different methods and samples have been used. Adopting the astrometric data and line-of-sight velocities of main sequence stars from *Gaia* DR2, we present a detailed analytical study of stellar kinematics in the solar neighborhood. Based on an improved version of the Strömberg relation, we obtain a robust estimation of the solar peculiar motion, which is given by $(U_\odot, V_\odot, W_\odot) = (8.63 \pm 0.64, 4.76 \pm 0.49, 7.26 \pm 0.36)\,\mathrm{km\,s^{-1}}$. The corresponding radial scalelength is yielded as $R_d \sim 2.5\,\mathrm{kpc}$. The radial and vertical components of solar peculiar motion are basically consistent with the classical values, while the tangential component is a few $\mathrm{km\,s^{-1}}$ smaller than most estimates in literature.

**Key words:** astrometry — Galaxy: fundamental parameters — stars: kinematics and dynamics

## 1 INTRODUCTION

The local standard of rest (LSR) provides a fundamental reference framework for research on stellar kinematics in the Milky Way. The LSR is defined as the Milky Way's rotation speed traced by a hypothetical set of stars having perfectly circular orbits at the solar position. Converting observed kinematic data from the heliocentric system to the Galactocentric system requires explicit knowledge of the solar velocity with respect to the LSR, which is called the solar peculiar motion. Determination of the LSR corresponds to measurement of the solar peculiar motion $(U_\odot, V_\odot, W_\odot)$, where $U_\odot$ is the solar peculiar velocity in the direction of the Galactic Center (GC), $V_\odot$ in the direction of Galactic rotation and $W_\odot$ in the direction of the North Galactic Pole (NGP).

The estimate of $U_\odot$ in previous research ranges from $\sim 6\,\mathrm{km\,s^{-1}}$ to $\sim 12\,\mathrm{km\,s^{-1}}$ and $W_\odot$ from $\sim 5\,\mathrm{km\,s^{-1}}$ to $\sim 9\,\mathrm{km\,s^{-1}}$ (Aumer & Binney 2009; Zhu 2009; Schönrich et al. 2010; Bobylev & Bajkova 2014; Tian et al. 2015; Bobylev 2017; Bobylev & Bajkova 2017). Compared to $U_\odot$ and $W_\odot$, the estimation for $V_\odot$ is much more debatable, varying from around $3\,\mathrm{km\,s^{-1}}$ (Golubov et al. 2013) to around $26\,\mathrm{km\,s^{-1}}$ (Bovy et al. 2012). The main problem in determination of $V_\odot$ is the correction of asymmetric drift $V_\mathrm{a}$, which is the difference in velocity of the LSR, i.e. $v_\mathrm{LSR}$, and the measured mean rotational velocity of the stellar sample, i.e. $\bar{v}_\phi$. The relation between $V_\mathrm{a}$ and $V_\odot$ is summarized by $V_\mathrm{a} = v_\mathrm{LSR} - \bar{v}_\phi = \Delta V - V_\odot$, where $\Delta V$ is the tangential velocity of the Sun with respect to the stellar group considered. For stellar populations that have approximately reached dynamical equilibrium, the asymmetric drift increases with increasing velocity dispersion (Dehnen & Binney 1998; Binney & Tremaine 2008).

The usual approach for measuring $V_\odot$ is twofold. The first approach makes use of cold disk objects (i.e. newborn objects such as masers, O-B stars and open clusters): the velocity of the LSR can be roughly replaced by the mean rotational velocity of the objects so that asymmetric drift can be neglected, i.e. $V_\odot \simeq \Delta V$. In the work of Zhu (2009), the author analyzed the first-order velocity space of 301 open clusters and obtained $V_\odot = 13.3 \pm 0.5\,\mathrm{km\,s^{-1}}$, coupled with the circular velocity of the clusters, $235 \pm 10\,\mathrm{km\,s^{-1}}$. On the contrary, the second method relies on late-type stars presenting significant velocity dispersion that can be used to disentangle the asymmetric drift. In the classical work of Dehnen & Binney (1998), the authors investigated both the first and second velocity moments of *Hipparcos* main sequence stars and constrained asymmetric drift using the Strömberg relation. The tangential peculiar motion was estimated by fitting the Strömberg relation to kinematic data of the sampled stars, which gave $V_\odot = 5.25 \pm 0.62\,\mathrm{km\,s^{-1}}$ (Dehnen & Binney 1998).

In a strict sense, values of the solar peculiar motion obtained from the above two methodologies are not consistent. On the one hand, even the youngest observed populations have velocity dispersion of $\sim 10\,\mathrm{km\,s^{-1}}$ (Aumer & Binney 2009, McMillan & Binney 2010, Ding et al. 2017), indicating that the disk traced by these objects cannot be absolutely "cold." In this case, the value of $V_\odot$ obtained with the first approach has an offset of around a few $\mathrm{km\,s^{-1}}$, which makes $V_\odot$ larger than that derived from the second approach. On the other hand, some substructures such as the spiral arm (Soubiran et al. 2003; De Simone et al. 2004; Quillen & Minchev 2005) and the warp (Miyamoto et al. 1988; Miyamoto & Zhu 1998; Poggio et al. 2017; Poggio et al. 2018) may distort the rotation of young populations that are not well-relaxed in the disk, but they have less impact on late-type stars (Dehnen & Binney 1998; Zhu 2000). Therefore, the second approach provides a more proper estimation for the solar peculiar motion.

In this work, we re-determine the LSR using the astrometric data and line-of-sight velocities from the second *Gaia* data release (DR2, Gaia Collaboration et al. 2018b). *Gaia* DR2 has provided the most complete and accurate kinematic data at this stage, which is of great help for us to investigate stellar kinematics in the solar neighborhood. Introducing a new version of the Strömberg relation proposed by Golubov et al. (2013), we make a robust measurement of the solar peculiar motion. Section 2 lays out the data sampling. In Section 3, we analyze the stellar kinematics and determine the solar peculiar motion. Section 4 concludes with a discussion.

## 2 DATA USED

The *Gaia* DR2 catalog (Gaia Collaboration et al. 2018b) has provided high-precision measurements of positions, parallaxes and proper motions for 1.3 billion sources. The median uncertainty in parallax is about 0.04 mas for bright ($G < 14$ mag) sources, 0.1 mas at $G = 17$ mag and 0.7 mas at $G = 20$ mag; for proper motions, the corresponding uncertainties are 0.05, 0.2 and $1.2\,\mathrm{mas\,yr^{-1}}$, respectively (Lindegren et al. 2018). The systematics in the parallaxes are generally below 0.1 mas and the bias of the parallax zeropoint is around 0.03 mas (Lindegren et al. 2018). *Gaia* DR2 contains line-of-sight velocities for 7.2 million stars with effective temperature in the range between 3550 K and 6900 K, which provide full sky coverage (Cropper et al. 2018; Gaia Collaboration et al. 2018a; Katz et al. 2018). The overall precision of the line-of-sight velocities is $1.05\,\mathrm{km\,s^{-1}}$, and the line-of-sight velocity residuals with respect to ground-based surveys are at a level of $0.1\,\mathrm{km\,s^{-1}}$ (Katz et al. 2018).

We select stars with measurements of both astrometry and line-of-sight velocity. According to the *Gaia* DR2 catalog, sources with duplicate sources or which are identified and processed as variables are rejected. We only retain stars with excess noise $\epsilon_i < 1$ and with the longest semi-major axis of the 5-D error ellipsoid smaller than 1 mas to obtain more reliable analysis of stellar kinematics. Considering the accuracy of velocity moments derived using the astrometric data, only stars with small relative parallax uncertainties $\sigma_p/\tilde{p} < 0.1$ are retained. The spatial coverage is restricted to $1/\tilde{p} < 0.3\,\mathrm{kpc}$ and the color scale is confined to $0 < (\mathrm{BP}-\mathrm{RP})_0 < 1$.

Figure 1 gives the color-magnitude diagram (CMD) of the selected stars according to the above criteria. We obtain the main sequence stars using the cuts in Figure 1. Finally, a total number of $N = 295\,293$ stars remain.

## 3 DETERMINATION OF THE LSR

### 3.1 Stellar Kinematics

The determination of the LSR calls for a detailed analysis of the first and second velocity moments of different stellar populations. We describe the stellar motions in the heliocentric Cartesian coordinate system $(u, v, w)$ such that the $u$-axis points to the GC, $v$-axis in the direction of Galactic rotation and $w$-axis to the NGP. The first velocity moment is parameterized by solar motion with respect to the mean velocity of the stellar population considered, i.e. $(\Delta U, \Delta V, \Delta W)$. The second velocity moment, also called the velocity ellipsoid, is denoted by a dispersion tensor $\boldsymbol{D_v}$. The tensor $\boldsymbol{D_v}$ contains six independent parameters $(\sigma_U, \sigma_V, \sigma_W, \rho_{uv}, \rho_{uw}, \rho_{vw})$, in which $\sigma_U^2$, $\sigma_V^2$ and $\sigma_W^2$ are the squared velocity dispersions in the directions $u$, $v$ and $w$ respectively, and the dimensionless parameters $\rho_{uv}$, $\rho_{uw}$, $\rho_{vw}$ stand for the correlation coefficients between velocities in every two directions.

With the measurements of astrometry and line-of-sight velocities, we employ and generalize the maximum likelihood (ML) method proposed by Aghajani & Lindegren (2013) to estimate the velocity moments $(\Delta U, \Delta V, \Delta W)$ and $\boldsymbol{D_v}$, taking into consideration the measurement uncer-

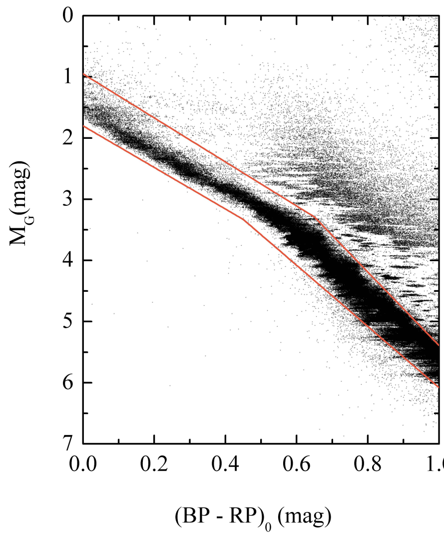


**Fig. 1** CMD of the selected stars from *Gaia* DR2, which satisfy $\epsilon_i < 1$, with the longest semi-major axis of the 5-D error ellipsoid smaller than 1 mas and $\sigma_p/\tilde{p} < 0.1$. The spatial coverage is restricted to 0.3 kpc from the Sun. The *polygonal lines* are used to identify the main sequence stars.

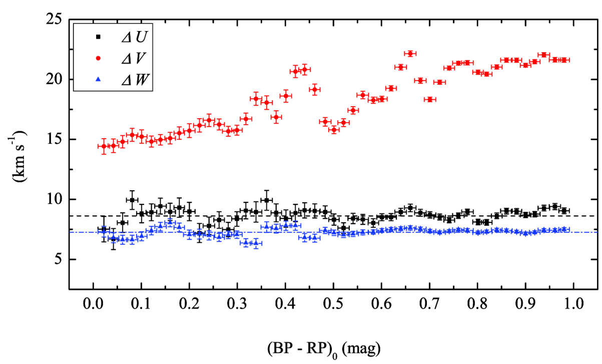


**Fig. 2** The solar motion with respect to the mean velocity of the group of stars considered as functions of stellar color: the *black squares*, *red circles* and *blue triangles* indicate the velocity components in the directions $u$, $v$ and $w$ respectively. The *black dashed line* and *blue dash-dotted line* mark $8.63\,\mathrm{km\,s^{-1}}$ and $7.26\,\mathrm{km\,s^{-1}}$ for the mean of $\Delta U$ and $\Delta W$ respectively.

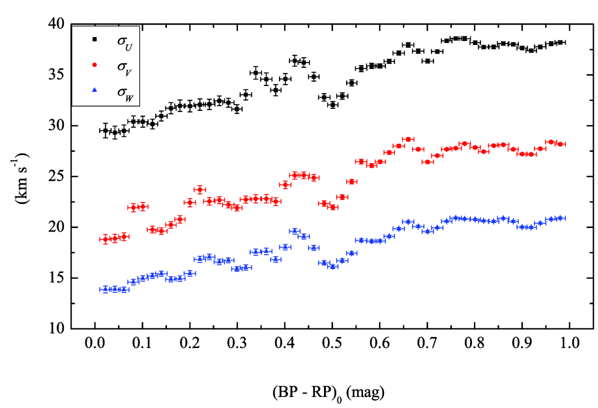


**Fig. 3** Same as Fig. 2, but for the radial (*black squares*), tangential (*red circles*) and vertical (*blue triangles*) components of velocity dispersion.

tainties (see Appendix). Figures 2–5 exhibit the estimates of velocity moments as a function of stellar color. The bin width is 0.04 mag in $(\mathrm{BP}-\mathrm{RP})_0$ and the bin's stepsize is 0.02 mag.

In Figure 2, the estimates of $\Delta U$ and $\Delta W$ are approximately consistent along stellar color with only a few fluctuations. Averaging the measurements of $\Delta U$ and $\Delta W$ separately, we have $U_\odot \simeq \langle \Delta U \rangle = 8.63 \pm 0.64\,\mathrm{km\,s^{-1}}$ and $W_\odot \simeq \langle \Delta W \rangle = 7.26 \pm 0.36\,\mathrm{km\,s^{-1}}$. As for $\Delta V$, the estimates generally increase with an increase in color index. Similarly, all the three components of velocity dispersion presented in Figure 3 have an uptrend toward later-type stars. The relation between $\Delta V$ and dispersion components provides information about asymmetric drift, which will be adopted to constrain the solar peculiar motion in the next subsection.

Figure 4 shows the axial ratios of the velocity ellipsoid. The mean of $\sigma_V^2/\sigma_U^2$ is found to be $0.499 \pm 0.049$, which agrees well with the prediction from epicyclic theory (i.e. $\sigma_V^2/\sigma_U^2 \simeq 0.5$) for a galaxy with a flat rotation curve (Evans & Collett 1993; Dehnen & Binney 1998). The ratios $\sigma_W^2/\sigma_U^2$ yield a mean of $0.268 \pm 0.025$, which is in keeping with the theoretical value 0.25 for a classical Kepler potential (Wielen 1977; Ida et al. 1993; Shiidsuka & Ida 1999). It is notable that both the ratios increase slightly toward later-type stars. The ratio $\sigma_V^2/\sigma_U^2$ is related to the slope of the Milky Way's rotation curve: for a mean streaming velocity that is declining outward with Galactocentric radius, the typical $\sigma_V^2/\sigma_U^2$ is less than 0.5, while an increase in stellar streaming velocity toward the outer disk leads to a ratio greater than 0.5 (Evans & Collett 1993). On the other hand, the ratio $\sigma_W^2/\sigma_U^2$ can be used to trace the secular heating process in the disk, which is mainly produced by molecular clouds scattering (Nordström et al. 2004; Smith et al. 2012). Therefore, the gradient with stellar color provides (weak) indication that later-type stars are more affected by the heating from molecular clouds.

Figure 5 gives the deviation angles of the principal axis for the velocity ellipsoid, which are deduced using $\rho_{uv}$, $\rho_{uw}$ and $\rho_{vw}$

$$\alpha_{ij} = \frac{1}{2} \arctan\left(\frac{2\rho_{ij}\sigma_i\sigma_j}{\sigma_i^2 - \sigma_j^2}\right), \tag{1}$$

where $i,\, j = u, v, w$. The angle $\alpha_{uv}$ is the well-known vertex deviation, ranging from $5^\circ$ to $20^\circ$. The vertex deviation can be interpreted by both the influence of a spiral (Soubiran et al. 2003; De Simone et al. 2004; Quillen & Minchev 2005; Levine et al. 2006) and a weak distortion in the Galaxy's potential, which could be attributed

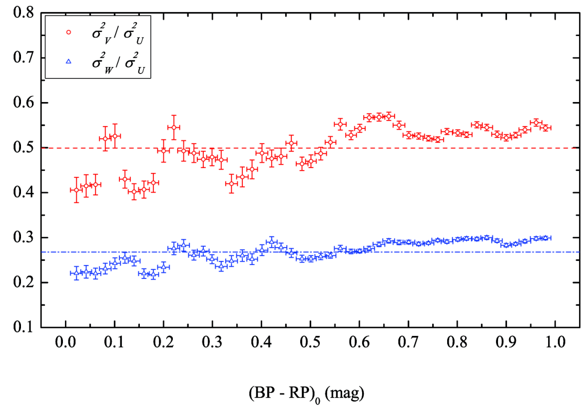


**Fig. 4** Same as Fig. 2, but for the squared dispersion ratios $\sigma^2_V/\sigma^2_U$ (*red circles*) and $\sigma^2_W/\sigma^2_U$ (*blue triangles*). The *red dashed line* and *blue dash-dotted line* mark 0.499 and 0.268 for the mean of $\sigma^2_V/\sigma^2_U$ and $\sigma^2_W/\sigma^2_U$ respectively.

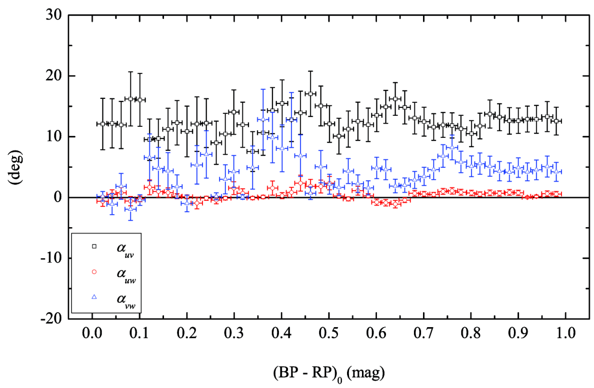


**Fig. 5** Same as Fig. 2, but for the deviation angles of the principal axis of the velocity ellipsoid in the $(u,\, v)$ (*black squares*)-, $(u,\, w)$ (*red circles*)- and $(v,\, w)$ (*blue triangles*)-planes.

to a central bar or a triaxial halo (Pont et al. 1994; Dwek et al. 1995; Kuijken 1996; Minchev et al. 2010; Gerhard 2016). In contrast to the notable $\alpha_{uv}$, the value of $\alpha_{uw}$ is nearly vanishing, which is in agreement with the recent findings that the velocity ellipsoid tilt approaches zero at the Galactic plane (Binney et al. 2014; Büdenbender et al. 2015). The estimates of $\alpha_{vw}$ indicate weak coupling between the tangential and vertical velocities, which is probably due to the warp in the solar neighborhood. It has been found that the warping motion is like a rotation with an axis pointing to the GC (Zhu 2000; Bobylev 2010).

### 3.2 Estimating the Solar Peculiar Motion

In this subsection, we focus on the estimation of $V_\odot$. The velocity dispersion ratios shown in Figure 4 indicate that the sampled stars have approximately reached dynamical-equilibrium. The stability of $\Delta U$, $\Delta W$ and the velocity ellipsoid deviation shown in Figures 2 and 5 implies that the stars are well-relaxed in the solar vicinity. Under these circumstances, the sample is appropriate for disentangling the asymmetric drift. The classical Strömberg relation addresses a linear relationship between $\Delta V$ and $\sigma^2_U$, which calls for a constant shape of the velocity ellipsoid (Dehnen & Binney 1998; Golubov et al. 2013). However, we have found in Figure 4 that the axial ratios of the velocity ellipsoid are not constant. In order to constrain $V_\odot$ accurately, we adopt a new robust Strömberg relation proposed by Golubov et al. (2013), which was derived from the Jeans equation (Binney & Tremaine 2008). In the Galactocentric cylindrical system $(R,\, \phi,\, z)$, the new Strömberg relation is written as

$$\Delta V' = V_\odot - \frac{V_\odot^2}{2v_\odot} + \frac{\sigma_R^2}{k}, \tag{2}$$

with

$$\Delta V' \equiv \Delta V + \frac{\sigma_R^2 + \eta(\sigma_R^2 - \sigma_z^2) - \sigma_\phi^2 - \Delta V^2}{2v_\odot}. \tag{3}$$

In Equations (2) and (3), $v_\odot$ denotes the solar rotational velocity, i.e., $v_\odot = v_{\rm LSR} + V_\odot$. We employ the proper motion of Sgr A* along Galactic longitude, i.e., $\mu_{\rm SgrA*} = (-6.379 \pm 0.026)\,{\rm mas\,yr^{-1}}$ (Reid & Brunthaler 2004) and obtain $v_\odot = 252.2\,{\rm km\,s^{-1}}$ by using $R_0 = 8.34\,{\rm kpc}$ (Reid et al. 2014). The dimensionless parameter $\eta$ describes the orientation of the principal axis of the velocity ellipsoid above and below the Galactic plane, i.e. $R\partial\sigma_{Rz}/\partial z = \eta(\sigma_R^2 - \sigma_z^2)$. Thus $\eta = 0$ corresponds to a horizontal orientation of the principal axis and $\eta = 1$ to a spherical orientation. Since it has been reported that the velocity ellipsoid shows a spherical orientation in the solar neighborhood (Siebert et al. 2008; Smith et al. 2012; Binney et al. 2014; Büdenbender et al. 2015), we adopt $\eta = 1$ for definiteness. The parameter $k$, which is proportional to the radial scalelength $R_d$, is a constant in Equation (2). Considering that our sample is confined to the solar vicinity, we analyze the asymmetric drift at $R = R_0$ and have $\sigma_R^2 \simeq \sigma_U^2$ and $\sigma_\phi^2 \simeq \sigma_V^2$.

The values of $\Delta V'$ derived from Equation (3) are shown in Figure 6, which increase linearly along with $\sigma_U^2$. Fitting Equation (2) to the data in Figure 6, we obtain $V_\odot = 4.76 \pm 0.49\,{\rm km\,s^{-1}}$, together with $1/k = 0.0131 \pm 0.0004\,{\rm km^{-1}\,s}$. Adopting the relation $k = v_\odot R_d/R_0$ (Golubov et al. 2013), the radial scalelength is derived as $R_d \sim 2.5\,{\rm kpc}$.

Figure 6 also gives the estimation in the case of a horizontal orientation of the velocity ellipsoid (i.e. $\eta = 0$) as a comparison, which yields $V_\odot = 4.45 \pm 0.49\,{\rm km\,s^{-1}}$ and $R_d \sim 2.8\,{\rm kpc}$. Obviously a horizontal orientation leads to

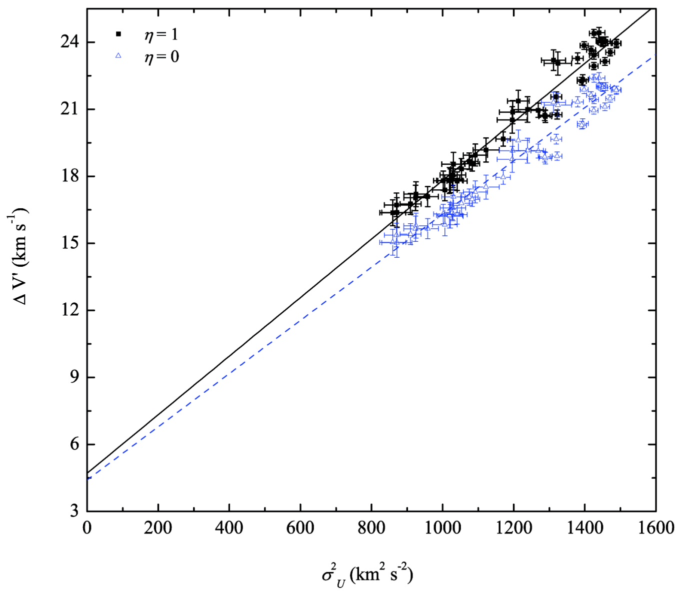


**Fig. 6** Value of $\Delta V'$ as a function of $\sigma_U^2$. The *black squares* indicate the data points derived in the case of $\eta = 1$ and the *blue triangles* signify the case $\eta = 0$. The *black solid line* and *blue dashed line* give the linear best fits in the cases of $\eta = 1$ and $\eta = 0$ respectively. (*Color online*).

**Table 1** Determinations of the solar peculiar motion in recent literature and in the current work.

| Reference | $U_\odot$ (km s$^{-1}$) | $V_\odot$ (km s$^{-1}$) | $W_\odot$ (km s$^{-1}$) | Stellar sample |
|---|---|---|---|---|
| Bobylev & Bajkova (2007) | $8.7 \pm 0.5$ | $6.2 \pm 2.2$ | $7.2 \pm 0.8$ | FG dwarfs |
| Aumer & Binney (2009) | $9.96 \pm 0.33$ | $5.25 \pm 0.54$ | $7.07 \pm 0.34$ | *Hipparcos* main sequence stars |
| Francis & Anderson (2009) | $7.5 \pm 1.0$ | $13.5 \pm 0.3$ | $6.8 \pm 0.1$ | Local *Hipparcos* stars with known radial velocities |
| Reid et al. (2009) | 9 | 20 | 10 | VLBI masers |
| Zhu (2009) | $11.7 \pm 0.6$ | $13.3 \pm 0.5$ | $8.1 \pm 0.6$ | Galactic open clusters |
| Bobylev & Bajkova (2010) | $5.5 \pm 2.2$ | $11 \pm 1.7$ | $8.5 \pm 1.2$ | VLBI masers |
| Breddels et al. (2010) | $12.0 \pm 0.6$ | $20.4 \pm 0.5$ | $7.8 \pm 0.3$ | RAVE DR2 stars |
| Schönrich et al. (2010) | $11.1^{+0.69}_{-0.75}$ | $12.24^{+0.47}_{-0.47}$ | $7.25^{+0.37}_{-0.36}$ | *Hipparcos* main sequence stars |
| Coşkunoğlu et al. (2011) | $8.50 \pm 0.29$ | $13.38 \pm 0.43$ | $6.49 \pm 0.26$ | RAVE thin disk dwarfs |
| Bovy et al. (2012) | $10 \pm 1$ | $26 \pm 3$ | | APOGEE red clump and red giant branch |
| Golubov et al. (2013) | $8.74 \pm 0.13$ | $3.06 \pm 0.68$ | $7.57 \pm 0.07$ | RAVE dwarfs |
| Bobylev & Bajkova (2014) | $6.0 \pm 0.5$ | $10.6 \pm 0.8$ | $6.5 \pm 0.3$ | O-B2.5 stars, masers and Cepheids |
| Reid et al. (2014) | $9.9 \pm 3.0$ | $14.6 \pm 5.0$ | $9.3 \pm 1.0$ | VLBI masers |
| Sharma et al. (2014) | $10.96^{+0.14}_{-0.13}$ | $7.53^{+0.16}_{-0.16}$ | $7.539^{+0.095}_{-0.09}$ | RAVE stars |
| Huang et al. (2015) | $7.01 \pm 0.20$ | $10.13 \pm 0.12$ | $4.95 \pm 0.09$ | LAMOST FGK main sequence stars |
| Huyan et al. (2015) | | $8.0 \pm 1.2$ | | ACAD FG stars |
| Tian et al. (2015) | $9.58 \pm 2.39$ | $10.52 \pm 1.96$ | $7.01 \pm 1.67$ | LAMOST FGK main sequence stars |
| Bobylev & Bajkova (2016) | $9.12 \pm 0.10$ | $20.80 \pm 0.10$ | $7.66 \pm 0.08$ | RAVE DR4 stars |
| Huang et al. (2016) | | $12.1 \pm 7.6$ | | Primary red clump giants and halo K giants |
| Bobylev (2017) | $7.90 \pm 0.65$ | $11.73 \pm 0.77$ | $7.39 \pm 0.62$ | *Gaia* DR1 classical Cepheids |
| Bobylev & Bajkova (2017) | $8.19 \pm 0.74$ | $9.28 \pm 0.92$ | $8.79 \pm 0.74$ | *Gaia* DR1 OB stars |
| This work | $8.63 \pm 0.64$ | $4.76 \pm 0.49$ | $7.26 \pm 0.36$ | *Gaia* DR2 main sequence stars |

a larger asymmetric drift compared to a spherical orientation.

## 4 DISCUSSION AND CONCLUSIONS

In this work, we have analyzed the kinematics of nearby main sequence stars and re-determined the LSR, using astrometric data and measurements of line-of-sight velocities from the recently released *Gaia* DR2 catalog. Table 1 presents different determinations of the solar peculiar motion in recent literature.

The measurements of $V_\odot$ derived by different samples are debatable, with discrepancies as large as $20\,\mathrm{km\,s^{-1}}$ (see Table 1). Fitting the robust Strömberg relation to kinematic data of the sampled stellar populations, the best-fit $V_\odot$ obtained in this work is around $7.5\,\mathrm{km\,s^{-1}}$ smaller than the classical determination of Schönrich et al. (2010). Figure 3 shows that all the sampled populations have radial velocity dispersion $\gtrsim 30\,\mathrm{km\,s^{-1}}$, indicating that these populations are dynamically hot. It is noteworthy that the Jeans equation, which produces the robust Strömberg relation, only holds in populations with pronounced velocity dispersions, since the dynamically cold populations are easily distorted by regional non-axisymmetric substructures such as a spiral arm (Quillen & Minchev 2005; Levine et al. 2006; Siebert et al. 2012). The sample used in Schönrich et al. (2010) contains dynamically cold *Hipparcos* stars. These stars could be involved in the spiral pattern or dissolving clusters, and thus make a difference in the determination of the LSR. Since there is no universal model to precisely correct for the kinematical deviation caused by regional perturbations so far, the populations with low random velocities, which could lead to kinematical bias, are unfit for analyzing asymmetric drift. Thanks to the large sample size of *Gaia* DR2, we obtain high-precision kinematic data for large amounts of dynamically hot populations in the solar vicinity to efficiently determine the LSR.

In Table 1, it is notable that the discrepancy among the results of $U_\odot$, though much smaller than that for $V_\odot$, is significant compared to $W_\odot$. The non-negligible variation in $U_\odot$ could be due to the kinematical properties of some specific populations. For example, the rotation of some young objects is non-axisymmetric (Kuijken & Tremaine 1994; Metzger et al. 1998; Zhu 2008; Ding et al. 2017), which can lead to a visualized inside-out motion and create a larger $U_\odot$.

The slope of the linear fit in Figure 6 gives a radial scalelength of $\sim 2.5\,\mathrm{kpc}$ in the case of $\eta = 1$ as a byproduct. Using RAVE (Steinmetz & RAVE Collaboration 2005) dwarf stars, Golubov et al. (2013) found from the new Strömberg relation that $R_d$ varies from around 1.6 kpc for metal-rich stars to around 2.9 kpc for metal-poor stars. Moreover, Robin et al. (2003) demonstrated that the radial scalelengths of a thick disk with age 11 Gyr and a thin disk with age $> 0.15$ Gyr are around 2.5 kpc, but the young thin disk has a much larger scalelength. The radial scalelength represents the property of stellar distribution in the disk, such that a less centrally concentrated distribution of stars gives a larger $R_d$. Our result is generally consistent with the estimates for long-lived disk stars in literature. More kinematic data of different Galactic objects will help to improve constraints on the structure and evolution of the Milky Way.

With the development of research on Galactic kinematics and dynamics, such as constraints on the rotation curve, the measurements of aberration of Galactic objects (Liu et al. 2013; Butkevich & Lindegren 2014) and the studies of mixing processes such as radial migration (Kordopatis et al. 2015; López-Corredoira & González-Fernández 2016), an explicit and robust determination of the LSR is more important than in the past, especially the in-plane components of the solar peculiar motion. In this work, we have re-determined the LSR by exploiting the kinematics of selected *Gaia* DR2 stars. Further improvement in the accuracy and completeness of astrometric and spectroscopic data will help us to further our understanding of the Milky Way.

**Acknowledgements** This work has made use of data from the European Space Agency (ESA) mission *Gaia* (`https://www.cosmos.esa.int/gaia`), processed by the *Gaia* Data Processing and Analysis Consortium (DPAC, `https://www.cosmos.esa.int/web/gaia/dpac/consortium`). Funding for the DPAC has been provided by national institutions, in particular the institutions participating in the *Gaia* Multilateral Agreement. This work is funded by the National Natural Science Foundation of China (Grant Nos. 11833004 and 11473013). We wish to thank the anonymous referee for useful comments and suggestions which helped to improve the manuscript.

## Appendix A: ESTIMATING THE VELOCITY MOMENTS BASED ON THE MAXIMUM LIKELIHOOD METHOD

Using high-precision astrometric data and line-of-sight velocities, the first and second velocity moments can be obtained simultaneously with ML estimation. ML estimation is extended based on the method formulated by Aghajani & Lindegren (2013).

We set $\tilde{p}$, $\tilde{\mu}_{\alpha*}$, $\tilde{\mu}_\delta$ and $\tilde{v}_{\rm los}$ to be the observed parallax, proper motions and line-of-sight velocity. The observational uncertainties of $\tilde{p}$, $\tilde{\mu}_{\alpha*}$, $\tilde{\mu}_\delta$ and $\tilde{v}_{\rm los}$ are all taken into consideration. The systematic errors in parallaxes are neglected, since the sample used in this work extends only to 0.3 kpc from the Sun and the systematics ($< 0.1$ mas, Lindegren et al. 2018) have little impact on our analysis. As for the line-of-sight velocities, it has been reported that their residuals with respect to different ground-based surveys do not exceed a few 100 $\mathrm{m\,s^{-1}}$ (Katz et al. 2018), which makes the (probable) systematic errors in $\tilde{v}_{\rm los}$ also meaningless in this estimation.

The velocity moments are summarized as $\boldsymbol{\theta} = (\Delta U,\, \Delta V,\, \Delta W,\, \boldsymbol{D_v})$ (see Sect. 3). When the true parallax $p$ is known, the observed velocity of one star is written as $\tilde{\boldsymbol{v}} = (\kappa\tilde{\mu}_{\alpha*}/p,\, \kappa\tilde{\mu}_\delta/p,\, \tilde{v}_{\rm los})^{\rm T}$, where $\kappa = 4.74047$ if the units for velocities, proper motions and parallaxes are $\rm km\ s^{-1}$, $\rm mas\ yr^{-1}$ and mas, respectively.

Taking into consideration the observational uncertainty of the parallax, we have the log-likelihood function of one star

$$L(\boldsymbol{\theta}, p) = \ln f_{\tilde{\boldsymbol{v}}}(\tilde{\boldsymbol{v}}|\boldsymbol{\theta},\, p) + \ln g(\tilde{p} - p), \tag{A.1}$$

where $f_{\tilde{\boldsymbol{v}}}(\tilde{\boldsymbol{v}}|\boldsymbol{\theta},\, p)$ is the conditional probability density function (pdf) of $\tilde{\boldsymbol{v}}$ when $p$ is known, and $g$ is the centered normal pdf of the observed parallax $\tilde{p}$ with standard uncertainty $\sigma_p$.

The key point is to obtain the formulation of $f_{\tilde{\boldsymbol{v}}}(\tilde{\boldsymbol{v}}|\boldsymbol{\theta},\, p)$. Set $\boldsymbol{v}$ to be the expected velocity of a star and $\boldsymbol{C}_{\tilde{\boldsymbol{v}}}$ to be the corresponding covariance matrix formulated by both the dispersion tensor $\boldsymbol{D_v}$ and the observational uncertainties (see below). Since both the velocity distribution and observational uncertainties are approximately Gaussian, the pdf $f_{\tilde{\boldsymbol{v}}}(\tilde{\boldsymbol{v}}|\boldsymbol{\theta},\, p)$ is written as

$$\begin{aligned} f_{\tilde{\boldsymbol{v}}}(\tilde{\boldsymbol{v}}|\boldsymbol{\theta},\, p) =& (2\pi)^{-\frac{3}{2}} \left|\boldsymbol{C}_{\tilde{\boldsymbol{v}}}\right|^{-\frac{1}{2}} \\ & \times \exp\left[-\frac{1}{2}(\tilde{\boldsymbol{v}} - \boldsymbol{v})^{\rm T} {\boldsymbol{C}_{\tilde{\boldsymbol{v}}}}^{-1} (\tilde{\boldsymbol{v}} - \boldsymbol{v})\right]. \end{aligned} \tag{A.2}$$

Now we give the expressions of $\boldsymbol{v}$ and $\boldsymbol{C}_{\tilde{\boldsymbol{v}}}$ using the rotation matrixes. Applying the definition $\boldsymbol{\Delta v} = (\Delta U,\, \Delta V,\, \Delta W)^{\rm T}$, we have

$$\boldsymbol{v} = -\boldsymbol{M_2 M_1 \Delta v}. \tag{A.3}$$

Both $M_1$ and $M_2$ are $3 \times 3$ matrixes

$$\boldsymbol{M}_1 = \begin{pmatrix} -\sin l & \cos l & 0 \\ -\sin b \cos l & -\sin b \sin l & \cos b \\ \cos b \cos l & \cos b \sin l & \sin b \end{pmatrix}, \tag{A.4}$$

where $(l,\, b)$ is the Galactic coordinate of the star;

$$\boldsymbol{M}_2 = \begin{pmatrix} \cos\psi & \sin\psi & 0 \\ -\sin\psi & \cos\psi & 0 \\ 0 & 0 & 1 \end{pmatrix}, \tag{A.5}$$

where $\psi$ is the star position angle that can be calculated via

$$\begin{aligned} \cot\psi \;=\; & -\cot i_N \cos\delta \sec(\alpha - \alpha_N) \\ & -\sin\delta \tan(\alpha - \alpha_N), \end{aligned} \tag{A.6}$$

in which $i_N = 62.8717°$ and $\alpha_N = 282.8595°$ (Liu et al. 2011).

The covariance $\boldsymbol{C}_{\tilde{\boldsymbol{v}}}$, resulting from both $\boldsymbol{D_v}$ and observational uncertainties, is in the following form

$$\begin{aligned} \boldsymbol{C}_{\tilde{\boldsymbol{v}}} =& \boldsymbol{M_2 M_1 D_v {M_1}^{\rm T} {M_2}^{\rm T}} \\ & + \begin{pmatrix} \kappa^2\sigma^2_{\mu_{\alpha*}}/p^2 & \kappa^2\rho\sigma_{\mu_{\alpha*}}\sigma_{\mu_\delta}/p^2 & 0 \\ \kappa^2\rho\sigma_{\mu_{\alpha*}}\sigma_{\mu_\delta}/p^2 & \kappa^2\sigma^2_{\mu_\delta}/p^2 & 0 \\ 0 & 0 & \sigma^2_{v_{\rm los}} \end{pmatrix}, \end{aligned} \tag{A.7}$$

where $\sigma_{\mu_{\alpha*}}$, $\sigma_{\mu_\delta}$ and $\sigma_{v_{\rm los}}$ are the observational uncertainties in $\tilde{\mu}_{\alpha*}$, $\tilde{\mu}_\delta$ and $\tilde{v}_{\rm los}$ respectively, and $\rho$ is the correlation coefficient between $\tilde{\mu}_{\alpha*}$ and $\tilde{\mu}_\delta$. Since only stars with $\sigma_p/\tilde{p} < 0.1$ are adopted in the analysis, the correlation between $\tilde{p}$ and $\tilde{\mu}_{\alpha*}$ or $\tilde{\mu}_\delta$ is negligible. In this case, the correlation between the proper motion and parallax is neglected.

Returning to Equation (A.1), the true parallax $p$ can be eliminated from it under the condition of small relative parallax errors (Aghajani & Lindegren 2013). The simplified log-likelihood function is

$$L(\boldsymbol{\theta}) \simeq \ln f_{\tilde{\boldsymbol{v}}}(\tilde{\boldsymbol{v}}|\boldsymbol{\theta},\, \tilde{p}) + \frac{1}{2}\sigma_p^2 F^2(\tilde{p}), \tag{A.8}$$

where $F(\tilde{p}) = \left(\partial \ln f_{\tilde{\boldsymbol{v}}}(\tilde{\boldsymbol{v}}|p)/\partial p\right)_{p=\tilde{p}}$.

Equation (A.8) is the log-likelihood function for one star and the total log-likelihood function for all stars in a sample is

$$L(\boldsymbol{\theta}) \simeq \sum_{i=1}^{N}\left[\ln f_{\tilde{\boldsymbol{v}},i}(\tilde{\boldsymbol{v}}_i|\boldsymbol{\theta}, \tilde{p}_i) + \frac{1}{2}\sigma^2_{p,i} F_i^2(\tilde{p}_i)\right], \tag{A.9}$$

where $N$ is the total number of stars considered. Using the Markov Chain Monte Carlo (MCMC) method (Metropolis et al. 1953), $\boldsymbol{\theta}$ can be estimated from the likelihood function in Equation (A.9).

## References


Aghajani, T., & Lindegren, L. 2013, A&A, 551, A9

Aumer, M., & Binney, J. J. 2009, MNRAS, 397, 1286

Binney, J., & Tremaine, S. 2008, Galactic Dynamics: Second Edition (Princeton: Princeton University Press)

Binney, J., Burnett, B., Kordopatis, G., et al. 2014, MNRAS, 439, 1231

Bobylev, V. V. 2010, Astronomy Letters, 36, 634

Bobylev, V. V. 2017, Astronomy Letters, 43, 152

Bobylev, V. V., & Bajkova, A. T. 2007, Astronomy Reports, 51, 372

Bobylev, V. V., & Bajkova, A. T. 2010, MNRAS, 408, 1788

Bobylev, V. V., & Bajkova, A. T. 2014, MNRAS, 441, 142

Bobylev, V. V., & Bajkova, A. T. 2016, Astronomy Letters, 42, 90

Bobylev, V. V., & Bajkova, A. T. 2017, Astronomy Letters, 43, 159

Bovy, J., Allende Prieto, C., Beers, T. C., et al. 2012, ApJ, 759, 131
Breddels, M. A., Smith, M. C., Helmi, A., et al. 2010, A&A, 511, A90
Büdenbender, A., van de Ven, G., & Watkins, L. L. 2015, MNRAS, 452, 956
Butkevich, A. G., & Lindegren, L. 2014, A&A, 570, A62
Coşkunoğlu, B., Ak, S., Bilir, S., et al. 2011, MNRAS, 412, 1237
Cropper, M., Katz, D., Sartoretti, P., et al. 2018, A&A, 616, A5
De Simone, R., Wu, X., & Tremaine, S. 2004, MNRAS, 350, 627
Dehnen, W., & Binney, J. J. 1998, MNRAS, 298, 387
Ding, P.-J., Zhu, Z., & Liu, J.-C. 2017, RAA (Research in Astronomy and Astrophysics), 17, 117
Dwek, E., Arendt, R. G., Hauser, M. G., et al. 1995, ApJ, 445, 716
Evans, N. W., & Collett, J. L. 1993, MNRAS, 264, 353
Francis, C., & Anderson, E. 2009, New Astron., 14, 615
Gaia Collaboration, Katz, D., Antoja, T., et al. 2018a, A&A, 616, A11
Gaia Collaboration, Brown, A. G. A., Vallenari, A., et al. 2018b, A&A, 616, A1
Gerhard, O. 2016, in IAU Symposium, 317, The General Assembly of Galaxy Halos: Structure, Origin and Evolution, eds. A. Bragaglia, M. Arnaboldi, M. Rejkuba, & D. Romano, 266
Golubov, O., Just, A., Bienaymé, O., et al. 2013, A&A, 557, A92
Huang, Y., Liu, X.-W., Yuan, H.-B., et al. 2015, MNRAS, 449, 162
Huang, Y., Liu, X.-W., Yuan, H.-B., et al. 2016, MNRAS, 463, 2623
Huyan, Z.-B., Zhu, Z., & Liu, J.-C. 2015, RAA (Research in Astronomy and Astrophysics), 15, 393
Ida, S., Kokubo, E., & Makino, J. 1993, MNRAS, 263, 875
Katz, D., Sartoretti, P., Cropper, M., et al. 2018, arXiv:1804.09372
Kordopatis, G., Binney, J., Gilmore, G., et al. 2015, MNRAS, 447, 3526
Kuijken, K. 1996, in Astronomical Society of the Pacific Conference Series, 91, IAU Colloq. 157: Barred Galaxies, eds. R. Buta, D. A. Crocker, & B. G. Elmegreen, 504
Kuijken, K., & Tremaine, S. 1994, ApJ, 421, 178
Levine, E. S., Blitz, L., & Heiles, C. 2006, Science, 312, 1773
Lindegren, L., Hernández, J., Bombrun, A., et al. 2018, A&A, 616, A2
Liu, J.-C., Zhu, Z., & Hu, B. 2011, A&A, 536, A102
Liu, J.-C., Xie, Y., & Zhu, Z. 2013, MNRAS, 433, 3597
López-Corredoira, M., & González-Fernández, C. 2016, AJ, 151, 165
McMillan, P. J., & Binney, J. J. 2010, MNRAS, 402, 934
Metropolis, N., Rosenbluth, A. W., Rosenbluth, M. N., Teller, A. H., & Teller, E. 1953, J. Chem. Phys., 21, 1087
Metzger, M. R., Caldwell, J. A. R., & Schechter, P. L. 1998, AJ, 115, 635
Minchev, I., Boily, C., Siebert, A., & Bienayme, O. 2010, MNRAS, 407, 2122
Miyamoto, M., Yoshizawa, M., & Suzuki, S. 1988, A&A, 194, 107
Miyamoto, M., & Zhu, Z. 1998, AJ, 115, 1483
Nordström, B., Mayor, M., Andersen, J., et al. 2004, A&A, 418, 989
Poggio, E., Drimmel, R., Smart, R. L., Spagna, A., & Lattanzi, M. G. 2017, A&A, 601, A115
Poggio, E., Drimmel, R., Lattanzi, M. G., et al. 2018, MNRAS, 481, L21
Pont, F., Mayor, M., & Burki, G. 1994, A&A, 285, 415
Quillen, A. C., & Minchev, I. 2005, AJ, 130, 576
Reid, M. J., & Brunthaler, A. 2004, ApJ, 616, 872
Reid, M. J., Menten, K. M., Zheng, X. W., et al. 2009, ApJ, 700, 137
Reid, M. J., Menten, K. M., Brunthaler, A., et al. 2014, ApJ, 783, 130
Robin, A. C., Reylé, C., Derrière, S., & Picaud, S. 2003, A&A, 409, 523
Schönrich, R., Binney, J., & Dehnen, W. 2010, MNRAS, 403, 1829
Sharma, S., Bland-Hawthorn, J., Binney, J., et al. 2014, ApJ, 793, 51
Shiidsuka, K., & Ida, S. 1999, MNRAS, 307, 737
Siebert, A., Bienaymé, O., Binney, J., et al. 2008, MNRAS, 391, 793
Siebert, A., Famaey, B., Binney, J., et al. 2012, MNRAS, 425, 2335
Smith, M. C., Whiteoak, S. H., & Evans, N. W. 2012, ApJ, 746, 181
Soubiran, C., Bienaymé, O., & Siebert, A. 2003, A&A, 398, 141
Steinmetz, M., & RAVE Collaboration. 2005, in Bulletin of the American Astronomical Society, 37, American Astronomical Society Meeting Abstracts, 1367
Tian, H.-J., Liu, C., Carlin, J. L., et al. 2015, ApJ, 809, 145
Wielen, R. 1977, A&A, 60, 263
Zhu, Z. 2000, PASJ, 52, 1133
Zhu, Z. 2008, ChJAA (Chin. J. Astron. Astrophys.), 8, 96
Zhu, Z. 2009, RAA (Research in Astronomy and Astrophysics), 9, 1285